PHYSICAL REVIEW A VOLUME 44, NUMBER 5 1 SEPTEMBER 1991

# Intensity correlation functions of the laser with multiplicative white noise

K. J. Phillips, M. R. Young, and Surendra Singh
*Department of Physics, University of Arkansas, Fayetteville, Arkansas 72701*
(Received 11 January 1991)

Two-time intensity correlations in a laser with multiplicative white noise have been studied experimentally. Multiplicative noise was introduced by applying a Gaussian-noise voltage to an intracavity acousto-optic modulator in a He:Ne laser operating near threshold. We observe both a shift and a broadening of the peak in the correlation-time versus mean-light-intensity curve. These observations are in agreement with the previous measurements of the steady-state properties of the laser near threshold in the presence of multiplicative noise.

## I. INTRODUCTION

The primary source of noise in lasers is spontaneous emission. This noise together with the nonlinearity of light-matter interaction determines the fluctuation properties of laser light [1]. In practice, however, other sources of noise also contribute to fluctuations of laser light. Since lasers are open systems coupled to their environment, random fluctuations of the environment also influence the statistical properties of laser light. These fluctuations of the environment enter the laser via pump or loss fluctuations. Noise due to these fluctuations is proportional to the electric-field amplitude in the lowest-order approximation. This type of noise is called multiplicative noise [2]. It is also referred to as parametric noise or external noise.

Lasers are but one example of open systems that are subject to multiplicative noise. The role of multiplicative noise in such systems has been of great interest recently [2,3]. The presence of multiplicative noise induces qualitatively new phenomena that cannot be induced by additive noise, white or colored, alone. It may cause the appearance of new statistically favored states. It may cause the shift of oscillation threshold. Many of these predictions have been confirmed experimentally in a variety of systems [4–7]. In a He:Ne laser, for example, the effects of multiplicative white noise have been investigated systematically in photoelectric counting experiments [5]. These experiments confirm the predicted shift of laser threshold and enhanced intensity fluctuations in the presence of multiplicative noise. The importance of multiplicative noise in lasers was realized when the statistical properties of dye lasers were investigated experimentally [7]. Experiments revealed that the observed intensity fluctuations could be accounted for only by including multiplicative noise, in addition to the additive spontaneous emission noise, in the equation of motion for the laser field amplitude [8]. Early theoretical work on dye lasers had predicted that the complex structure of dye molecules may alter the nature of nonlinearity [9]. In particular, the presence of triplet state absorption in the same spectral region as the singlet laser emission may induce a first-order phase-transition-like behavior in dye-laser fluctuations. This has, however, not been observed. It is not clear what role, if any, triplet absorption does play. Experiments that have been carried out to date seem to suggest that triplet states do not play an essential role. This conclusion can only be tentative since many of the effects induced by multiplicative noise are similar to those that would be induced by triplet absorption [9]. Effects of multiplicative noise and triplet absorption could be delineated in experiments that study the role of multiplicative noise in a systematic way by varying the strength of multiplicative noise in a controlled fashion. Such experiments have not been carried out in dye lasers. In simple systems, such as a He:Ne laser, systematic studies of the effects of multiplicative noise have been carried out by Young and Singh [5]. In these experiments the steady-state intensity fluctuations were studied in photoelectric counting experiments. Corresponding experimental studies of the effects of multiplicative noise on the correlation functions of laser light have not yet been reported although this problem has been treated theoretically by several workers [6,10,11]. In this paper we wish to describe results of photoelectric correlation experiments carried out on a He:Ne laser where multiplicative white noise was introduced in controlled amounts by applying a Gaussian-noise voltage to an intracavity acousto-optic modulator. The paper is organized as follows. In Sec. II we briefly review the steady-state fluctuation properties of a laser with multiplicative noise. We include both quantum noise due to spontaneous emission and multiplicative noise due to loss fluctuations. Section III discusses steady-state correlation functions of the laser. Experimental setup and procedures are described in Sec. IV. Finally, experimental results and principal conclusions are presented in Sec. V. Although both gain and loss fluctuations may contribute to multiplicative noise in lasers we confine ourselves to the case where loss fluctuations dominate. In the first approximation, especially when external fluctuations are small, both gain and loss fluctuations lead, qualitatively, to similar results.

## II. EQUATION OF MOTION

Consider a single-mode laser operating close to threshold whose losses are modulated by a white-noise Gaussian random process. The equation of motion for the scaled slowly varying complex field amplitude $E(t)$ of the laser can be written as [5,10-12]

$$\dot{E}(t)=E(t)[a-|E(t)|^2]+\eta(t)E(t)+q(t)\ , \tag{1}$$

where $q(t)$ is the spontaneous emission noise which is taken to be an additive Gaussian white-noise process with

$$\langle q(t)\rangle=0=\langle q^*(t)\rangle,\quad \langle q^*(t)q(t')\rangle=4\delta(t-t')\ . \tag{2}$$

Multiplicative noise due to loss fluctuations is taken to be another Gaussian white-noise process with

$$\langle \eta(t)\rangle=0=\langle \eta^*(t)\rangle,\quad \langle \eta^*(t)\eta(t')\rangle=4Q\delta(t-t') \tag{3}$$

and is assumed to be statistically independent of spontaneous emission noise $q(t)$. The average pump parameter $a$ can be expressed in terms of gain per pass $A$ and average loss per pass $C$ as [12]

$$a=\left[\frac{A}{C}-1\right]\sqrt{\pi}n_0\ , \tag{4}$$

where $n_0$ is the mean number of photons in the laser at threshold in the absence of multiplicative noise. Depending on the operating point of the laser the pump parameter may be negative, zero, or positive. Because of the presence of noise terms given by Eqs. (2) and (3) the laser field amplitude becomes a stochastic variable. Equation of motion (1) then has the form of a nonlinear stochastic equation which has no known analytic solution. It is convenient to replace the nonlinear stochastic equation (1) by a Fokker-Planck equation for the probability density $p(E,t)$ for the field amplitude to be characterized by value $E$ at the time $t$ [13]. This equation has the form

$$\frac{\partial p(E,t)}{\partial t}=-\frac{\partial}{\partial E}E(a-|E|^2)p(E,t)+2\frac{\partial^2}{\partial E\partial E^*}(1+Q|E|^2)p(E,t)+\text{c.c.}\ , \tag{5}$$

where in obtaining Eq. (5) from Eq. (1) we have interpreted the multiplicative noise term in the Stratonovich sense. This is because in our experiments multiplicative loss noise is not a true white-noise process. Instead it is a Gaussian-noise source with a very short correlation time. The steady-state solution of this equation satisfies $\dot{p}_s=0$. Solving Eq. (5) in the steady state with natural boundary conditions we find [5,10–12]

$$p_s(r)=\text{const}[r(1+Qr^2)^{\nu-1}e^{-r^2/2Q}]\ , \tag{6}$$

$$\nu=\frac{a}{2Q}+\frac{1}{2Q^2}\ , \tag{7}$$

for the steady-state probability density of amplitude $r$ and phase $\phi(E=re^{i\phi})$ of the laser. We note that the steady-state distribution (6) is independent of phase $\phi$. It depends only on the amplitude $r$. This means that in the steady state phase is uniformly distributed in the interval $0\le\phi\le2\pi$. Introducing light intensity $I=|E|^2$ we find the steady-state intensity distribution

$$P_s(I)=\text{const}[(1+QI)^{\nu-1}e^{-I/2Q}]\ , \tag{8}$$

for laser light. This is a single peaked distribution for all values of pump parameter $a$ and multiplicative noise strength $Q$. For a fixed value of $Q$ this distribution does not develop a nonzero maximum until $a>2Q$. This means that in the presence of multiplicative noise the laser threshold shifts from $a=0$ to $2Q$. Furthermore, distribution (8) is wider than the corresponding distribution for the ordinary laser. This implies that intensity fluctuations are enhanced when multiplicative noise is present in the laser. From Eq. (8) we obtain the following expressions for the mean light intensity $\langle I\rangle$ and normalized variance $\kappa_2$ of light intensity:

$$\langle I\rangle=a+\frac{e^{-1/2Q^2}}{(2Q^2)^{\nu-1}\Gamma(\nu,1/2Q^2)}\ , \tag{9}$$

$$\begin{aligned}\kappa_2&=\langle(I-\langle I\rangle)^2/\langle I\rangle^2\\&=\frac{a+2Q}{\langle I\rangle}+\frac{2}{\langle I\rangle^2}-1\ .\end{aligned} \tag{10}$$

Predictions of Eqs. (8)–(10) regarding steady-state fluctuations were tested in photoelectric counting measurements by introducing controlled amounts of multiplicative noise in a He:Ne laser [5]. These measurements provide a quantitative understanding of the role of multiplicative noise in determining the fluctuation properties of laser light. We now consider the time dependence of fluctuations in the steady state.

## III. TIME-DEPENDENT SOLUTION

In order to discuss the time-dependent solution we express the Fokker-Planck equation (5) in polar coordinates $r$, $\phi$ by writing

$$E=re^{i\phi},\quad 0\le r<\infty,\quad 0\le\phi<2\pi\ . \tag{11}$$

Then the probability density $p(r,\phi,t)$ of amplitude $r$ and phase $\phi$ satisfies

$$\dot{p}(r,\phi,t)=\left[-\frac{\partial}{\partial r}r\left[a-Q-r^2+\frac{1}{r^2}\right]+\frac{\partial}{\partial r}(1+Qr^2)\frac{\partial}{\partial r}+\left[\frac{1+Qr^2}{r^2}\right]\frac{\partial^2}{\partial\phi^2}\right]p(r,\phi,t)\ . \tag{12}$$

By using the method of separation of variables the general solution of Eq. (12) can be written in the form

$$p(r,\phi,t)=\sum_{n,l}C_{nl}e^{il\phi}g_{nl}(r)[p_s(r)]^{1/2}e^{-\lambda_{nl}t}\ , \tag{13}$$

where $0\le n<\infty$ and $-\infty<l<\infty$ are integers. The eigenvalues $\lambda_{nl}\ge0$ and the eigenfunctions $g_{nl}(r)$ are labeled by two indices because they satisfy a two-dimensional eigenvalue problem. Coefficients $C_{nl}$ are determined by the initial condition. The steady-state amplitude distribution is given by Eq. (6). Substituting Eq. (13) into Eq. (12) we obtain the eigenvalue equation

$$\frac{d}{dr}(1+Qr^2)\frac{d}{dr}g_{nl}+[\lambda_{nl}-F_l(r)]g_{nl}=0\ ,$$
$$F_l(r)=\frac{r^2}{4}\frac{(a-Q-r^2)^2}{1+Qr^2}+(a-Q-2r^2)-\frac{Qr^2(a-Q-r^2)}{2(1+Qr^2)}-\frac{Q}{4(1+Qr^2)}+Ql^2+\frac{l^2-\frac{1}{4}}{r^2}\ . \tag{14}$$

The lowest eigenvalue $\lambda_{00}=0$ corresponds to the steady-state solution. The corresponding eigenfunction is given by

$$g_{00}(r)=[p_s(r)]^{1/2}\ . \tag{15}$$

The eigenvalue equation (14) is a self-adjoint equation with boundary conditions $g_{nl}(r)\to 0$ as $r\to\infty$ and regular at the origin $r=0$. The eigenfunctions form an orthonormal complete set

$$\int_0^\infty dr\, g_{nl}(r)g_{n'l}(r)=\delta_{n,n'}\ , \tag{16}$$
$$\sum_{n=0}^{\infty}\sum_{l=-\infty}^{\infty} g_{nl}(r)g_{nl}(r')\frac{e^{il(\phi-\phi')}}{2\pi}=\delta(r-r')\delta(\phi-\phi')\ . \tag{17}$$

No analytic solutions for Eq. (14) are known. The eigenfunctions and eigenvalues are determined by numerical solution of Eq. (14). For this purpose Eq. (14) can be simplified further by making the substitution

$$g_{nl}(r)=\frac{\psi_{nl}}{(1+qr^2)^{1/2}}\ , \tag{18}$$

where $\psi_{nl}(r)$ satisfy the following equation:

$$(1+Qr^2)\frac{d^2\psi_{nl}}{dr^2}+[\lambda_{nl}-V_l(r)]\psi_{nl}=0\ , \tag{19}$$
$$V_l(r)=\frac{r^2}{4}\frac{(a-Q-r^2)^2}{1+Qr^2}+(a-2r^2)-\frac{Qr^2(a+Q-r^2)}{2(1+Qr^2)}-\frac{Q}{4(1+Qr^2)}+Ql^2+\frac{l^2-\frac{1}{4}}{r^2}\ . \tag{20}$$

This equation has the form of a radial Schrödinger equation for a particle with space-dependent mass.

In the steady-state single time averages are described by the distribution (6) and (7). In order to evaluate the multitime averages we need higher-order (multitime) probability densities. For our purpose the most important probability density is the second-order (two-time) probability density. In order to obtain this probability density we note that the solution with initial condition

$$p(r,\phi,t=0)=\delta(r-r_0)\delta(\phi-\phi_0) \tag{21}$$

is the Green's function or the conditional probability density $G(r,\phi,t|r_0,\phi_0,0)$ for the field to be characterized by amplitude and phase $r,\phi$ at time $t$ given that it was characterized by amplitude and phase $r_0$ and $\phi_0$ at $t=0$. Using Eqs. (13), (16), (17), and (21) we find

$$G(r,\phi,t|r_0,\phi_0,0)=\sum_{n=0}^{\infty}\sum_{l=-\infty}^{\infty}\frac{e^{il(\phi-\phi_0)}}{2\pi}g_{nl}(r)g_{nl}(r_0)\times e^{-\lambda_{nl}t}\frac{g_{00}(r)}{g_{00}(r_0)}\ . \tag{22}$$

If the initial state $p(r,\phi,t=0)$ is the steady-state $p_s(r,\phi)=g_{00}^2(r)/2\pi$ we find the two-time probability density $p_2(r,\phi,t;r_0,\phi_0,0)$ for the field to be characterized by $r,\phi$ at time $t$ and by $r_0$ and $\phi_0$ at time $t=0$ in the steady state. From Eqs. (17), (21), and (22) we find

$$p_2(r,\phi,t;r_0,\phi_0,0)=\sum_{n=0}^{\infty}\sum_{l=-\infty}^{\infty}\frac{e^{il\phi}}{2\pi}g_{nl}(r)g_{nl}(r_0)e^{-\lambda_{nl}t}\times g_{00}(r)g_{00}(r_0)\ . \tag{23}$$

Because we are dealing with a Markov process $E(t)$, all higher-order probability densities can be expressed in terms of the second-order (two-time) probability densities. For two-time intensity and field correlations we only need the second-order (two-time) probability density.

Once the two-time probability density is known we can calculate correlation functions. Thus for two-time field correlations we obtain

$$\langle E^*(t)E(t+\tau)\rangle=\int_0^\infty dr\int_0^\infty dr_0\int_0^{2\pi}d\phi\int_0^{2\pi}d\phi_0 rr_0 e^{i(\phi_0-\phi)}p_2(r,\phi,t;r_0,\phi_0,0)=\sum_{n=0}^{\infty}u_{n1}e^{-\lambda_{n1}\tau}\ , \tag{24}$$

where

$$u_{n1}=\left|\int_0^\infty dr\, rg_{00}(r)g_{n1}(r)\right|^2=\left|\int_0^\infty dr\, r\frac{\psi_{00}(r)\psi_{n1}(r)}{1+Qr^2}\right|^2 \tag{25}$$

and for two-time intensity correlations we obtain

$$\langle I(t)I(t+\tau)\rangle=\int_0^\infty dr\int_0^\infty dr_0\int_0^{2\pi}d\phi\int_0^{2\pi}d\phi_0 r^2r_0^2e^{i(\phi_0-\phi)}p_2(r,\phi,t;r_0,\phi_0,0)=\sum_{n=0}^{\infty}v_{n0}e^{-\lambda_{n0}\tau}\ , \tag{26}$$

where

$$v_{n0} = \left| \int_0^\infty dr\, r^2 g_{00}(r) g_{n0}(r) \right|^2$$
$$= \left| \int_0^\infty dr\, r^2 \frac{\psi_{00}(r)\psi_{n0}(r)}{1+Qr^2} \right|^2 . \quad (27)$$

It will be seen that for two-time correlations we need the eigenfunctions and eigenvalues of Eq. (19) with potentials $V_1$ and $V_0$. For large delays $\tau$ we expect the intensities $I(t)$ and $I(t+\tau)$ to be uncorrelated. This means that in the large delay time limit $\tau \to \infty$ the correlation function factorizes, $\langle I(t) I(t+\tau) \rangle \to \langle I \rangle^2 = v_{00}$. We can then write for the normalized correlation function $\mu(\tau)$ of intensity fluctuations $\Delta I(t) = I(t) - \langle I \rangle$ the following expression:

$$\mu(\tau) = \frac{1}{v_{00}} \sum_{n=1}^{\infty} v_{n0} e^{-\lambda_{n0}\tau} . \quad (28)$$

We note that at zero delay

$$\mu(0) = \langle (\Delta I)^2 \rangle / \langle I \rangle^2 \equiv \kappa_2 , \quad (29)$$

so that the value of the normalized correlation function at zero delay is simply the normalized variance $\kappa_2$ given by Eq. (9). From Eq. (29) we can define the intensity correlation time

$$T_c = \int_0^\infty d\tau \frac{\mu(\tau)}{\mu(0)} = \sum_{n=1}^{\infty} (v_{n0}/\lambda_{n0}) \Big/ \sum_{n=1}^{\infty} v_{n0} . \quad (30)$$

This time can be measured in experiments. Another quantity that is accessible to measurements is the effective eigenvalue $\lambda_{\text{eff}}$. This quantity is essentially the slope of the correlation function for short delays and characterizes the initial decay of correlations. For short delays we can write

$$\mu(\tau) \approx \mu(0) \left[ 1 - \tau \sum_{n=1}^{\infty} v_{n0}\lambda_{n0} \Big/ \sum_{n=1}^{\infty} v_{n0} \right]$$
$$\equiv \mu(0)(1 - \lambda_{\text{eff}}\tau) , \quad (31)$$

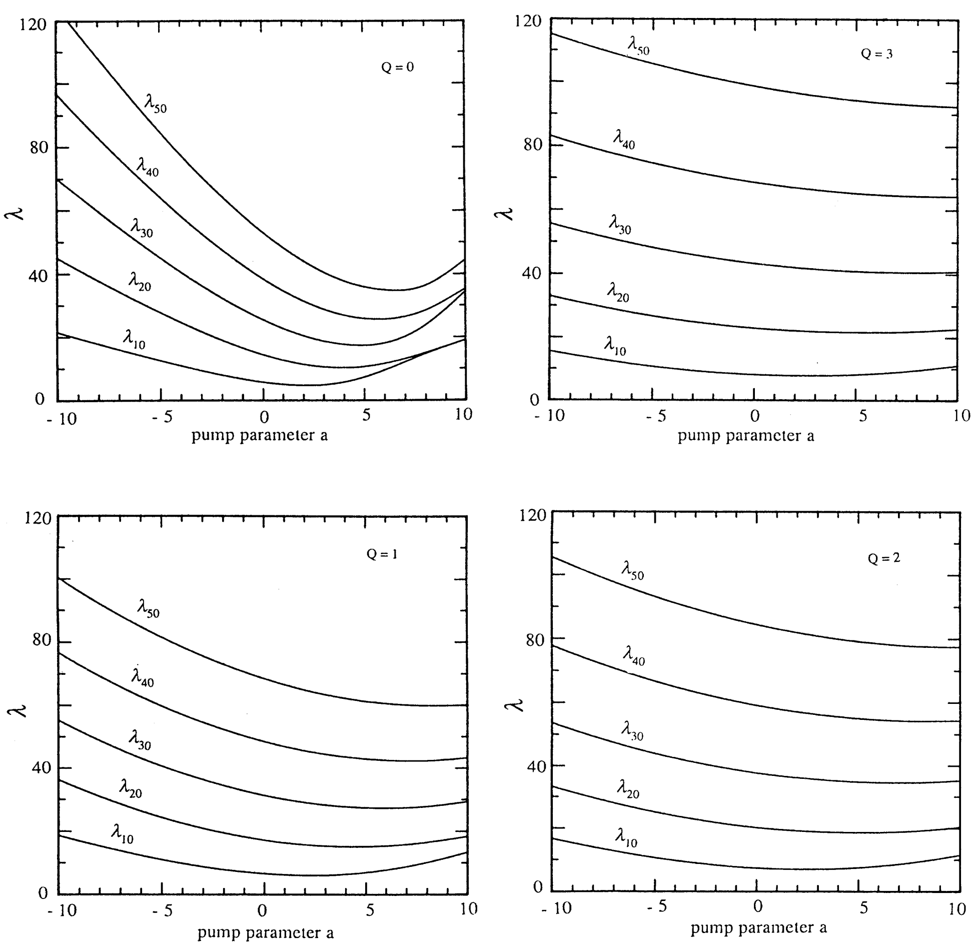


FIG. 1. Variation of the first few intensity eigenvalues $\lambda_{n0}$ with the pump parameter $a$ in the absence of multiplicative noise for several different values of multiplicative noise strength $Q$. Case $Q=0$ corresponds to the ordinary laser with no multiplicative noise.

which leads to the following expression for $\lambda_{\text{eff}}$:

$$\lambda_{\text{eff}} = \sum_{n=1}^{\infty} v_{n0}\lambda_{n0} \Big/ \sum_{n=1}^{\infty} v_{n0} \; . \tag{32}$$

Behavior of $T_c$ and $\lambda_{\text{eff}}$ has also been discussed by other workers [10,11,14] by using several different techniques. An exact expression for $\lambda_{\text{eff}}$ in terms of the steady-state moments of the light intensity can be derived based on the approach of San Miguel *et al.* [14]. For our case this leads to the following expression for $\lambda_{\text{eff}}$:

$$\lambda_{\text{eff}} = \frac{4\langle I\rangle(1+aQ+2Q^2)+8Q}{(a+2Q)\langle I\rangle+2-\langle I\rangle^2} \; . \tag{33}$$

This equation was used as a consistency check of our numerical results [Fig. (9)]. Our approach parallels the treatment of the ordinary single-mode laser. This method [15] is based on the fact that if Eq. (19) is integrated using some $\lambda \neq \lambda_{nl}$, the solution diverges exponentially as $r \to \infty$. Integration is ceased as soon as $\psi_{nl}(R)\psi'_{nl}(R) > 0$ for some value of $r = R$ such that $V_l(R) > \lambda$. The value of $\psi_{nl}$ at this point is recorded. This value $\psi_{nl}(R,\lambda)$ depends on $\lambda$. The problem of determining the eigenvalue $\lambda_{nl}$ then reduces to a search for a zero of $\psi_{nl}(R,\lambda)$. For numerical integration we used the Bulirsch-Stoer method [16]. The starting guesses for eigenvalues were the eigenvalues for the conventional laser. Once the eigenvalues and eigenfunctions are determined, the coefficients $v_{nl}$ were computed by using Eq. (27). Correlation time $T_c$ and the effective eigenvalues $\lambda_{\text{eff}}$ were measured in photoelectric correlation experiments and compared with the predictions of Eqs. (30) and (32). In

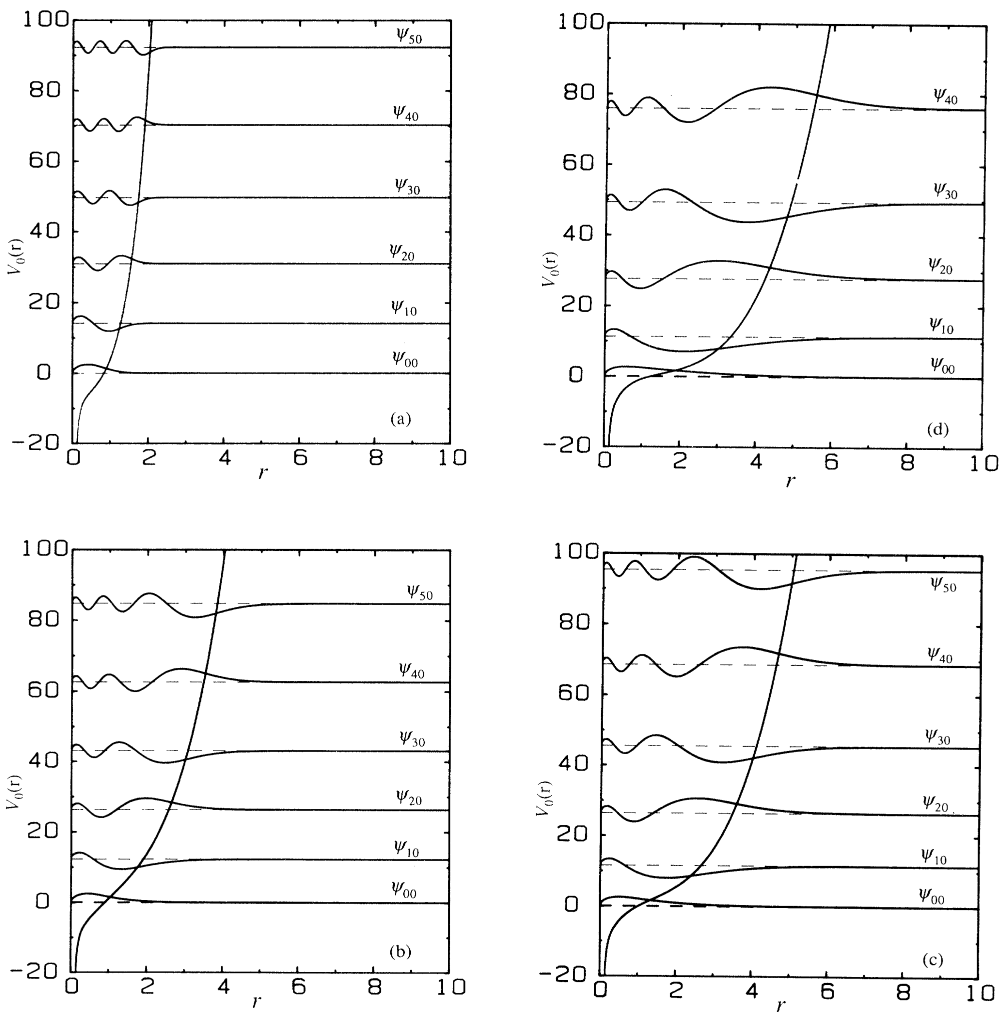


FIG. 2. The potential $V_0(r)$ of Eq. (20) and schematic forms of the first few eigenfunctions $\psi_{n0}(r)$ for $a=-6$ for increasing multiplicative noise strength: (a) $Q=0$, (b) $Q=1$, (c) $Q=2$, (d) $Q=3$. The dashed horizontal lines denote the corresponding eigenvalues.

the threshold region correlation functions cannot be approximated by a single exponential. In general several terms must be retained. Figure 1 shows the variation of the first few eigenvalues that occur in $\mu(\tau)$ with pump parameter $a$ for several different values of $Q$. Note that the lowest eigenvalue $\lambda_{00}=0$ corresponds to the steady state. One consequence of multiplicative noise is to lift the degeneracy of eigenvalues encountered in the ordinary laser ($Q=0$) near threshold. With increasing multiplicative noise strength the minima of eigenvalues near threshold become progressively shallower. The behavior of eigenfunctions $\psi_{nl}$ for $a=-6$ and 4 is shown in Figs. 2 and 3. From the eigenfunctions and eigenvalues we can calculate the intensity correlation time via Eqs. (27) and (30). Figure 4 shows the variation of correlation time with the strength $Q$ of multiplicative noise for several different values of pump parameter $a$. In the neighborhood of $a=0$ the correlation time always decreases as $Q$ increases. For large negative and positive values of $a$ the correlation time first increases slightly for small values of $Q$ and then decreases slowly as $Q$ is increased further.

## IV. EXPERIMENTAL SETUP

The experimental arrangement is shown in Fig. 5. It has been described in detail elsewhere [5,6]. A single-mode He:Ne laser was used in these experiments. Laser loss was modulated by applying a small amplitude Gaussian-noise voltage to an intracavity acousto-optic modulator (AOM). For small amplitudes of noise voltage the transfer characteristics of the AOM were linear. Loss

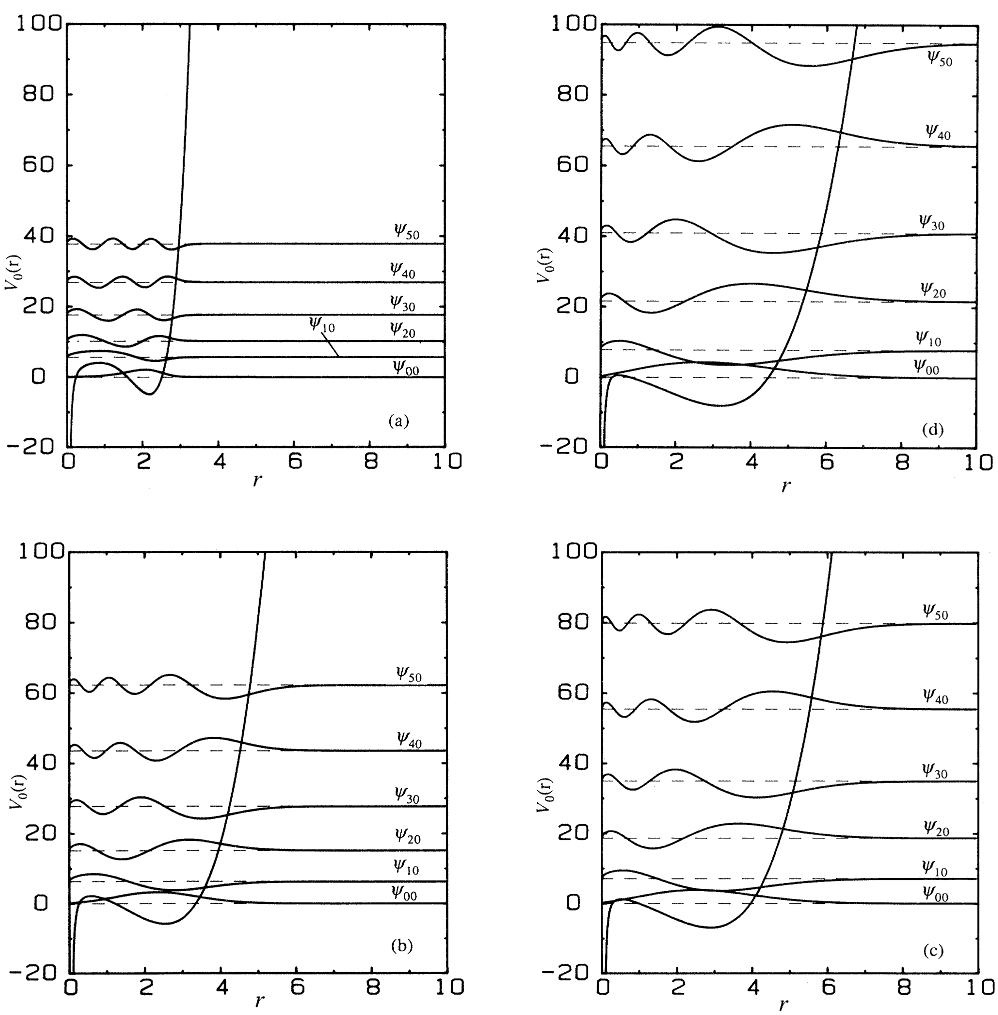


FIG. 3. The potential $V_0(r)$ of Eq. (20) and schematic forms of the first few eigenfunctions $\psi_{n0}(r)$ for $a=4$ for increasing multiplicative noise strength: (a) $Q=0$, (b) $Q=1$, (c) $Q=2$, (d) $Q=3$. The dashed horizontal lines denote the corresponding eigenvalues.

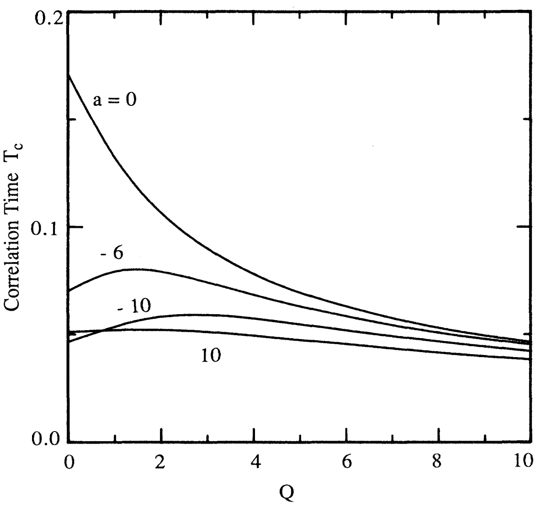


FIG. 4. Variation of the intensity correlation time with multiplicative noise strength $Q$ for several different values of the pump parameter $a$ in the neighborhood of threshold.

fluctuations were found to be Gaussian and their spectrum was flat within 2 dB up to 12 MHz. Because the correlation time associated with this bandwidth, $\sim 8$ ns, is small compared to the correlation time of the laser, $\sim 50$ $\mu$s, loss fluctuations can be approximated by a Gaussian white-noise source. The strength of multiplicative noise was varied by changing the rms amplitude of the noise voltage applied to the AOM. The laser operated in a single longitudinal and transverse mode with the cavity frequency tuned to line center with the help of a piezoelectric transducer (PZT). The entire assembly was enclosed in a temperature stabilized housing with acoustic isolation. Once thermal equilibrium was reached the laser was quite stable and frequency drifted less than 5 MHz over a period of several minutes. This time was long enough to make several measurements of correlation function. Operating point of the laser was varied with the help of a knife edge which was partially inserted into

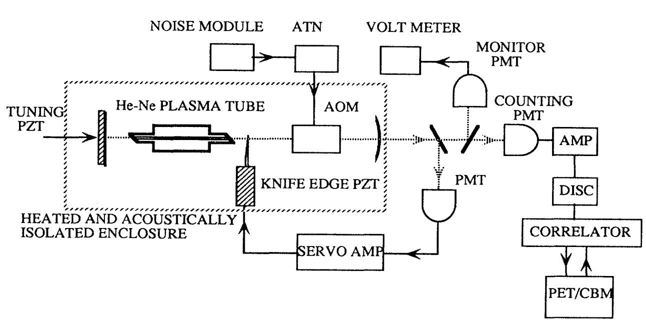


FIG. 5. An outline of the experimental setup. PET/CBM is PET microcomputer from Commodore Business Machines, AMP is amplifier, ATN is attenuator, and DISC is discriminator.

the beam inside the laser cavity. By pushing the knife edge in and out of the beam the net gain of the laser could be changed. The knife edge along with a photomultiplier tube monitoring a small portion of the beam emerging from the laser was part of an electronic feedback loop. The feedback loop could stabilize the laser intensity to better than 2% over the entire threshold region.

To perform the experiment a certain amount of noise voltage with appropriate attenuation was applied to the AOM. The laser was stabilized at some mean intensity by the feedback loop. The main beam of light coming out of the laser was allowed to fall on a fast high gain counting photomultiplier tube (PMT). The photoelectric pulses appearing at the output of the PMT were amplified and fed to a nonupdating discriminator. The discriminator produced standard rectangular pulses of amplitude $-750$ mV and duration 10 ns. The discriminator dead time, about 30 ns, was the longest dead time and, therefore, defined the system dead time for counting. The operation of the PMT and the counting electronics were checked by illuminating the PMT with light from a broadband thermal source. With a 2-$\mu$s counting time, which is large compared to the correlation time of thermal light, photoelectron statistics were found to be Poisson and measurements of correlation function produced a flat curve as expected. From the measured correlation function of thermal light the probability of after pulsing was found to be $<0.2\%$. Pulses from the discriminator were fed to a digital correlator operated in the autocorrelation mode. For each value of noise voltage applied to the AOM, several measurements of correlation function were made by varying the operating point of the laser. Each measurement consisted of $10^5$ samples and took approximately a minute to complete.

The correlator divides time into intervals of equal duration $\Delta\tau$. This time is referred to as sample time. In our experiments it was of the order of 2.5 $\mu$s. The number of pulses occurring during each sample time is counted by a shift register counter. At the end of each counting interval the counter shifts its contents into the first location of a 128-location store-and-shift register. At the end of the next counting interval the number in the first location is moved to the second location and the number in the counter is moved to the first location. This procedure is continued until all 128 channels are filled. From this stage on the same procedure is continued with the number in the last channel being discarded. Building of the correlation function now begins. At the receipt of each pulse by the counter the contents of each location in the store-shift register are added to the contents of corresponding memory location in the correlator memory. Thus at the end of a counting interval in which $n_i$ counts were recorded contents of memory location $j$ will increase by $n_i n_{i-j}$. After $N$ such samples the number in the $j$th channel will be

$$N_j = \sum_{i=1}^{N} n_i n_{i-j}, \quad j = 1, 2, \ldots, 128 \; . \tag{34}$$

For large number of samples $N$ we find that, for a stationary beam of light, the number in channel $j$ is related to the correlation function of light by

$$N_j=\alpha^2 N\int_0^{\Delta\tau}dt'\int_0^{\Delta\tau}dt''\langle I(t')I(t''-(j+1)\Delta\tau)\rangle \ . \quad (35)$$

Here $\alpha$ is the detector quantum efficiency. If the sample time $\Delta\tau$ is short compared with the correlation time of the laser we can approximate Eq. (35) by

$$N_j=\alpha^2(\Delta\tau)^2\langle I\rangle^2[1+\mu(j\Delta\tau)] \ . \quad (36)$$

This condition was very well satisfied in our experiments as $\Delta\tau\approx 2.5$ $\mu$s and the correlation time was of the order of 50 $\mu$s or greater. The correlator also records numbers in 16 channels corresponding to large delays that are of the order of $1028\Delta\tau$. Since for large delays no correlations survive, the numbers in these channels essentially give

$$N_\infty=\alpha^2(\Delta\tau)^2\langle I\rangle^2 \ . \quad (37)$$

Dividing Eq. (36) by Eq. (37) we obtain the normalized correlation function

$$\mu(j\Delta\tau)=\left[\frac{N_j}{N_\infty}-1\right] . \quad (38)$$

Note that the number in channel 1 does not correspond to $\mu(0)$. We also find that $\mu(\tau)$ given by Eq. (38) is independent of quantum efficiency of detection. Thus from measured values $N_j$ and $N_\infty$ we can extract the correlation function. In practice several corrections to data must be applied. First, not all the light falling on the photomultiplier tube is laser light. Background fluorescence from the plasma tube also contributes to pulses at the output of the PMT. If the background light is uncorrelated with the signal and its bandwidth is large compared to the inverse of the sample time the correlator results can be corrected readily for its effects. Let $I_L$ denote laser light intensity and $I_B$ denote background light intensity. Then by writing the total light intensity as the sum of laser light intensity and the background light intensity

$$I=I_L+I_B=I_L+\beta I \ , \quad (39)$$

with $\beta=I_B/I$ and using Eq. (39) in Eq. (35) we find that the true correlation function of laser light alone is given by

$$\mu(j\Delta\tau)=\frac{1}{(1-\beta)^2}\left[\frac{N_j}{N_\infty}-1\right] . \quad (40)$$

We must also correct for dead-time effects. Dead-time effects were quite small as the total count rate was kept below about 100 kilocounts per second by using some calibrated filters. With a dead-time ratio of $\approx 0.01$ dead-time corrections were found to be negligible and were not considered in these experiments. The stability of the laser during data acquisition was monitored by a photomultiplier tube. The output of this photomultiplier also served as a measurement of mean light intensity characterizing the operating point of the laser.

## V. EXPERIMENTAL RESULTS

A typical normalized correlation function is shown in Fig. 6. In order to extract correlation time from the measured correlation functions the data were fitted to a function of the form

$$\mu(\tau)=C_1e^{-\lambda_1\tau}+C_2e^{-\lambda_2\tau} \ , \quad (41)$$

which was found adequate to fit all correlation functions measured in the experiments. The method used for fitting the data is a nonlinear least-squares method due to Marquardt as implemented in an SAS subroutine [17]. The uncertainties in the fitted parameters were computed by assuming the numbers in various channels to be independent Poisson variates. From experimentally determined values of $C_1$, $C_2$, $\lambda_1$, and $\lambda_2$ we can extract various quantities that can be compared with theoretical predictions by

$$\mu(0)=C_1+C_2 \ , \quad (42)$$

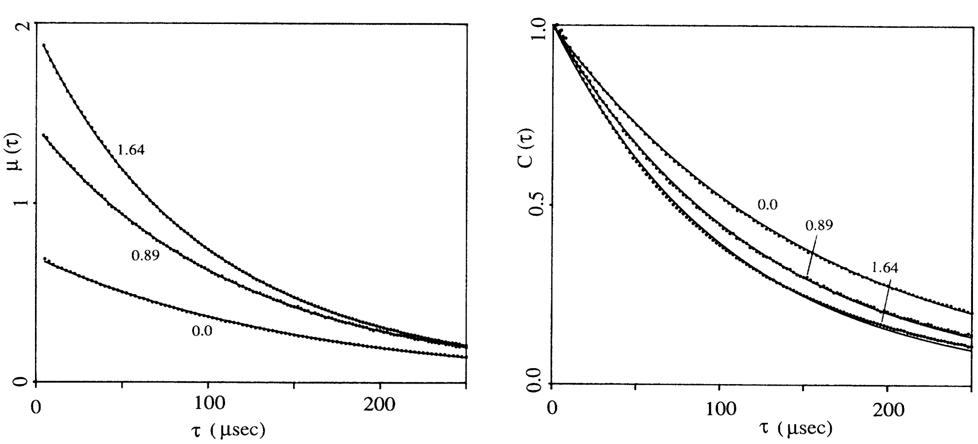


FIG. 6. Examples of measured normalized two-time intensity correlation functions. $\mu(\tau)$ is defined in Eq. (40) and $C(\tau)=\mu(\tau)/\mu(0)$. The dots represent experimental data and the solid curves are the best fits to the data.

$$T_c = \frac{1}{\mu(0)}\left[\frac{C_1}{\lambda_1}+\frac{C_2}{\lambda_2}\right], \tag{43}$$

$$\lambda_{\text{eff}} = \frac{1}{\mu(0)}(C_1\lambda_1 + C_2\lambda_2) . \tag{44}$$

The correlator does not give $\mu(0)$ because the first channel corresponds to a delay of $\Delta\tau = 2.5$ $\mu$s. For this reason $\mu(0) = \kappa_2$ was extracted by extrapolating the fitted function to zero delay.

In order to compare the experimental results with theoretical predictions we need to know the value of $Q$ and a scale factor that relates measured mean light intensity to the dimensional intensity used in theoretical calculations. The procedure for determining $Q$ was similar to that used in Refs. [5] and [6]. By plotting the normalized variance $\mu(0) = \kappa_2$ against mean light intensity on the $\log_{10}\langle I \rangle$ axis (Fig. 7), the measurements were compared with theoretical curves for several different values of $Q$. The required scale factor corresponds to a shift along the $\log_{10}\langle I \rangle$ axis. Value of $Q$ was determined by comparing the measured data with a series of $\kappa_2$ versus $\langle I \rangle$ curves. Another scale factor that relates measured times to dimensionless times was needed. This was determined by plotting the measured $T_c$ versus $\langle I \rangle$ curve on a $\log_{10}T_c$ axis. This scale factor corresponds to a shift along the time axis. For one value of noise voltage (and therefore $Q$) a single scale factor was needed as expected. Slightly different scale factors were needed for different values of $Q$.

Variation of the correlation time with mean light intensity is shown in Fig. 8 for several different values of multiplicative noise strength $Q$. The points represent experimental data and the solid curves are derived from Eq. (30). Curve $Q = 0$ corresponds to the ordinary laser without multiplicative noise. In all cases we find that the correlation time increases as excitation is increased at first. It reaches a maximum near threshold and decreases thereafter as mean light intensity increases. It is seen that the effect of multiplicative white noise is to decrease correlation time. This decrease is rapid first with increasing strength of multiplicative noise. Most dramatic decrease occurs near threshold. Away from threshold correlation time is relatively insensitive to the strength of multiplicative noise.

Variation of the effective eigenvalue which is the initial slope of the correlation function is shown in Fig. 9. Because the value of the correlation function at zero delay was not available we relied upon the fitted function to extract $\lambda_{\text{eff}}$ from the data via Eq. (44). This procedure seems justified because when the fitted function is extrapolated to zero delay we obtain $\kappa_2 = \mu(0)$ via Eq. (42). A comparison of $\kappa_2$ obtained by this procedure with theoretical predictions in Fig. 7 shows very good agreement. There is reasonable agreement between measured and predicted values of $\lambda_{\text{eff}}$. Note that $\lambda_{\text{eff}}$ depends only on the first few channels. However, the fitted function is affected by the fluctuations in the tail of the correlation function also. This may explain the slight discrepancy between the measured and predicted values of $\lambda_{\text{eff}}$. Behavior of $\lambda_{\text{eff}}$ is qualitatively similar to the behavior of $1/T_c$. As mean light intensity increases the initial slope of the correlation function decreases first, indicating a slow decay of correlations. It reaches a minimum near threshold and increases after that with increasing light intensity. The effect of multiplicative noise is to increase

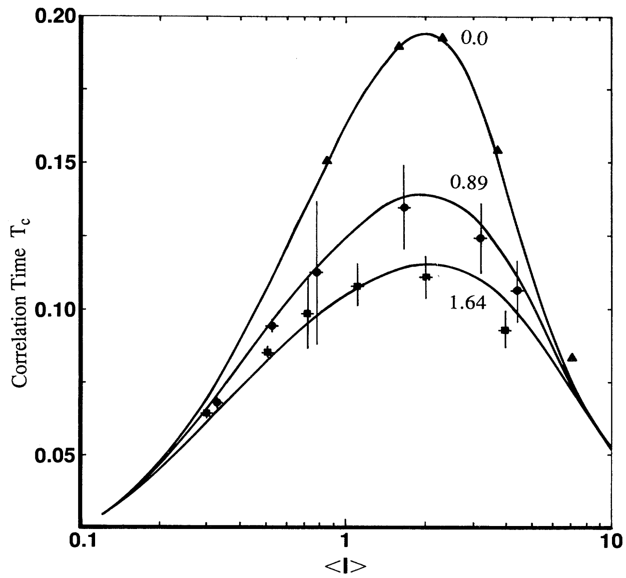


FIG. 8. A comparison of the measured intensity correlation time with the theoretical predictions for several different values of $Q$:$Q = 0.0$, 0.89, and 1.64. The solid circles represent experimental points and the continuous curves are theoretical predictions derived from Eq. (30).

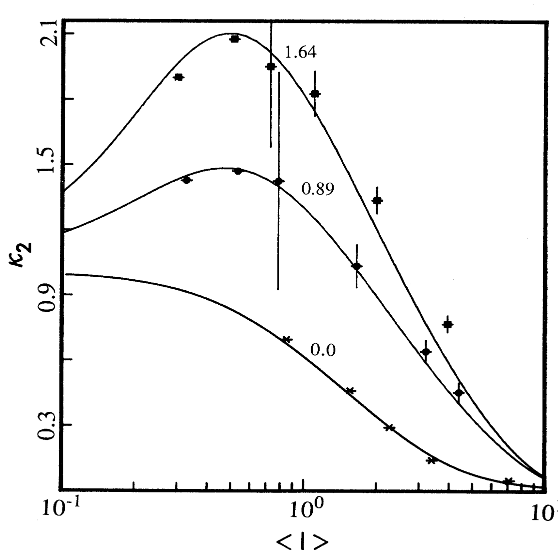


FIG. 7. Variation of the normalized intensity fluctuations $\kappa_2 = \langle(\Delta I)^2\rangle / \langle I \rangle^2 = \mu(0)$ with the pump parameter for $Q = 0.0$, 0.89, and 1.64. Experimentally, $\mu(0)$ was extracted by extrapolating the measured correlation functions (Fig. 6) to zero delay. The solid circles represent experimental points and the continuous curves are theoretical predictions derived from Eq. (10).

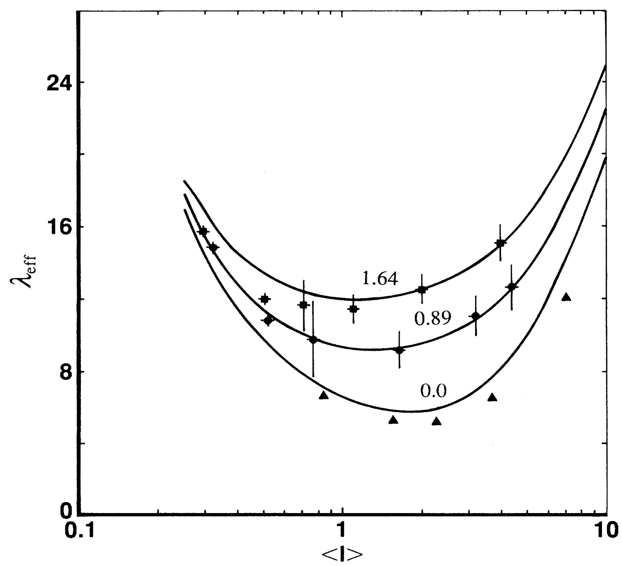


FIG. 9. A comparison of the measured initial slope $\lambda_{\rm eff}$ of the correlation functions with the theoretical predictions for several different values of $Q$: $Q=0.0$, 0.89, and 1.64. The solid circles represent experimental points and the continuous curves are theoretical predictions derived from Eq. (32). Predictions of Eq. (33) are indistinguishable from the continuous curve.

$\lambda_{\rm eff}$. This means multiplicative noise increases the rate of decay of correlations in the laser. Once again for small values of $Q$ we find a rapid increase in $\lambda_{\rm eff}$ as $Q$ is increased and this increase slows down as $Q$ is increased further. Far from threshold both $T_c$ and $\lambda_{\rm eff}$ are only weakly affected by the presence of multiplicative noise.

In the conventional single-mode laser intensity correlation time has a maximum near threshold. In the presence of multiplicative noise this maximum shifts very slowly to larger values of mean light intensity as multiplicative noise strength is increased. This shift is in agreement with a similar shift that was observed in the photoelectric counting measurements of the steady-state intensity distribution [5]. In these measurements it was found that the value of mean light intensity at which the steady-state intensity distribution exhibits a nonzero maximum for the first time increases with increasing multiplicative noise. Note that our definition of threshold corresponds to that used in the theory of oscillators [18]. Another effect associated with multiplicative noise is that the laser threshold transition becomes diffuse because the peak in the correlation time versus mean light intensity curve is relatively broad when multiplicative noise is present. We could not achieve higher multiplicative noise strengths in the experiments because for large noise voltages the transmission characteristics of the AOM were not linear. We were also limited by the small gain tube available for the experiments. Nevertheless we believe that we were able to access perhaps the most interesting regime in which the strengths of intrinsic and multiplicative noise are comparable. The presence of multiplicative noise changes laser characteristics significantly and this change is most pronounced for relatively small values of $Q\simeq 1$. For large values of $Q$ we do not expect qualitatively new features. At very high noise strengths and for high excitations some other issues may have to be addressed. For example, the assumption of a white-noise source for loss fluctuations may break down. In this case a model that incorporates a colored multiplicative noise source may be more appropriate [7]. In the region of threshold, however, with small amount of multiplicative noise the white-noise model seems to describe laser fluctuations quite well.

## ACKNOWLEDGMENTS

This work was supported by NSF Grants No. PHYS-8709528 and No. PHYS-88179532.


[1] H. Haken, in *Encyclopedia of Physics,* edited by S. Flugge (Springer-Verlag, Berlin, 1970), Vol. XXV/2C; M. Sargent III, M. O. Scully, and W. E. Lamb, Jr., *Laser Physics* (Addison-Wesley, Reading, MA, 1974); M. Lax, in *Brandeis Lectures,* edited by M. Chretien, E. P. Gross, and S. Deser (Gordon and Breach, New York, 1969); W. H. Louisell, *Quantum Statistical Properties of Radiation* (Wiley, New York, 1973).

[2] W. Horsthemke and R. Lefever, *Noise Induced Transitions* (Springer-Verlag, Berlin, 1984).

[3] F. Moss and L. A. Lugiato, *Noise and Chaos in Nonlinear Dynamical Systems* (Cambridge University Press, New York, 1989); F. Moss, *Noise in Nonlinear Dynamical Systems* (Cambridge University Press, New York, 1989).

[4] S. Kabashima, S. Kogure, T. Kawakubo, and T. Okada, J. Appl. Phys. **50**, 6296 (1979).

[5] M. R. Young and Surendra Singh, Opt. Lett. **13**, 21 (1988); Phys. Rev. A **38**, 238 (1988).

[6] A preliminary account of some of the results has appeared in K. J. Phillips and Surendra Singh, in *Coherence and Quantum Optics,* edited by J. H. Eberly, L. Mandel, and E. Wolf (Plenum, New York, 1990), pp. 915–919; see also M. R. Young, Ph.D. thesis University of Arkansas, 1987 (unpublished); K. J. Phillips, M. S. thesis, University of Arkansas, 1989 (unpublished).

[7] K. Kaminishi, R. Roy, R. Short, and L. Mandel, Phys. Rev. A **24**, 370 (1982); R. Short, L. Mandel, and R. Roy, Phys. Rev. Lett. **49**, 647 (1982); P. Lett, R. Short, and L. Mandel, *ibid.* **52**, 341 (1984); P. Lett, E. C. Gage, and Th. H. Chyba, Phys. Rev. A **35**, 746 (1987); T. H. Chyba, E. C. Gage, R. Ghosh, P. Lett, L. Mandel, and I. McMackin, Opt. Lett. **12**, 422 (1987).

[8] R. Graham, M. Hohnerbach, and A. Schenzle, Phys. Rev. Lett. **48**, 1396 (1983); S. M. Dixit and P. S. Sahni, *ibid.* **50**, 1273 (1983); R. F. Fox, G. F. James, and R. Roy, *ibid.* **52**, 1178 (1984); K. Lindberg, B. J. West, and E. Cortes, Appl. Phys. Lett. **44**, 175 (1984); P. Jung and H. Risken, Phys. Lett. **103A**, 38 (1984); A. Hernandez-Machado, M. San

Miguel, and S. Katz, Phys. Rev. A **31**, 2362 (1985); F. de Pasquale, J. M. Sancho, M. San Miguel, and P. Tartaglia, Phys. Rev. Lett. **56**, 2473 (1986).

[9] R. B. Schaefer and C. R. Willis, Phys. Rev. A **13**, 1874 (1976); A. Baczynski, A. Kossakowski, and T. Marzalek, Z. Phys. B **23**, 205 (1976); S. T. Dembinski and A. Kossakowski, *ibid.* **24**, 141 (1976); S. T. Dembinski, A. Kossakowski, and L. Wolniewicz, *ibid.* **27**, 281 (1977).

[10] A. Schenzle and H. Brand, Phys. Rev. A **20**, 1628 (1979); R. Graham and A. Schenzle, *ibid.* **26**, 1676 (1982).

[11] P. Jung, Th. Lieber, and H. Risken, Z. Phys. B **66**, 397 (1987).

[12] Surendra Singh, S. Friberg, and L. Mandel, Opt. Lett. **1**, 99 (1982); Phys. Rev. A **27**, 381 (1983); Surendra Singh, Phys. Rep. **108**, 217 (1984).

[13] J. Risken, *The Fokker-Planck Equation* (Springer-Verlag, Berlin, 1984).

[14] M. San Miguel, L. Pesquera, M. A. Rodriguez, and A. Hernandez-Machado, Phys. Rev. A **35**, 208 (1987).

[15] A. P. French and E. F. Taylor, *An Introduction to Quantum Physics* (Norton, New York, 1978), Chaps. 4 and 5; R. Merrill, Am. J. Phys. **40**, 138 (1972).

[16] R. Bulirsch and J. Stoer, Numerische Math. **8**, 1 (1966).

[17] D. W. Marquardt, J. Soc. Ind. Appl. Math. **11**, 431; SAS Institute, Inc., *SAS User's Guide: Statistics,* Version 5 Edition (SAS Institute, Inc., Cary, NC, 1985), pp. 575ff.

[18] R. L. Stratonovich, *Topics in the Theory of Random Noise* (Gordon and Breach, New York, 1963), Vol. II.